

RESTORE: Towards Feature Shift for Vision-Language Prompt Learning

Yuncheng Yang¹, Chuyan Zhang¹, Zuopeng Yang², Yuting Gao³, Yulei Qin³,
Ke Li³, Xing Sun³, Jie Yang¹, and Yun Gu¹

¹ Shanghai Jiao Tong University

Yaphabates@sjtu.edu.cn

² Guangzhou University

³ Tencent YouTu Lab

Abstract. Prompt learning is effective for fine-tuning foundation models to improve their generalization across a variety of downstream tasks. However, the prompts that are independently optimized along a single modality path, may sacrifice the vision-language alignment of pre-trained models in return for improved performance on specific tasks and classes, leading to poorer generalization. Existing work does not take such drawbacks into serious consideration, for the simple reason that the evaluation of visual and textual alignment for general purposes is excluded in experiments. In this paper, we first demonstrate that prompt tuning along only one single branch of CLIP (e.g., language or vision) is the reason why the misalignment occurs. Without proper regularization across the learnable parameters in different modalities, prompt learning violates the original pre-training constraints inherent in the two-tower architecture. To address such misalignment, we first propose feature shift, which is defined as the variation of embeddings after introducing the learned prompts, to serve as an explanatory tool. We dive into its relation with generalizability and thereafter propose RESTORE, a multi-modal prompt learning method that exerts explicit constraints on cross-modal consistency. To be more specific, in order to prevent feature misalignment, a feature shift consistency is introduced to synchronize inter-modal feature shifts by measuring and regularizing the magnitude of discrepancy during prompt tuning. In addition, we propose a "surgery" block to avoid short-cut hacking, where cross-modal misalignment can still be severe if the feature shift of each modality varies drastically at the same rate. It is implemented as feed-forward adapters upon both modalities to alleviate the misalignment problem. Extensive experiments on 15 datasets demonstrate that our method outperforms the state-of-the-art prompt tuning methods without compromising feature alignment. Codes and models are available at https://github.com/Yaphabates/RESTORE_.

Keywords: Prompt Learning · Vision Language Model · Feature Shift

1 Introduction

Vision-Language Models (VLMs) [23, 43] have demonstrated remarkable generalization capabilities across multiple tasks. The CLIP [43] is pre-trained on 400

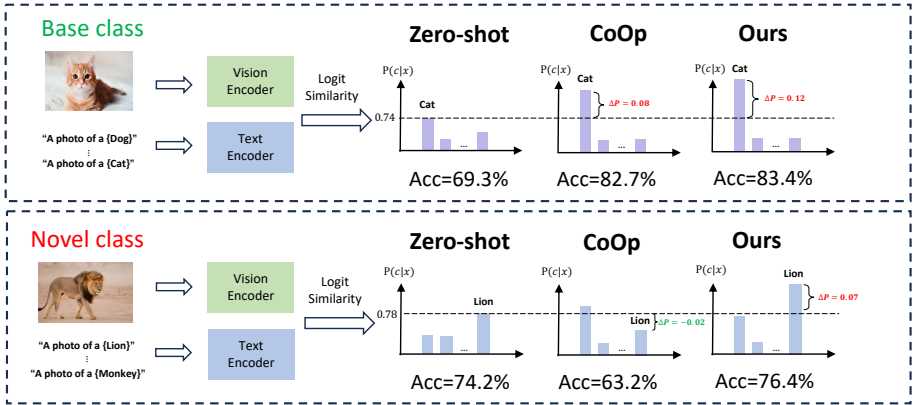


Fig. 1: The pre-trained VLM (e.g., CLIP) demonstrates a strong generalizability by its zero-shot performance on both base and novel classes. However, existing prompt learning methods over-emphasize performance gains on the seen base classes while ignoring their declining generalization on novel ones, which is demonstrated by the decreased probability $P(c|x)$ of the ground-truth category and the overall accuracy.

million pairs of images and texts with numerous computing resources, and it is impractical to conduct full parameter fine-tuning of the entire model for downstream tasks due to the high cost of collecting manually annotated large datasets with similar scale. For efficient tuning with smaller datasets and fewer trainable parameters, **prompt tuning** [24, 31, 73], **lightweight adapters** [32, 69, 70], and **low-rank parametric bypass matrices** [20] have been investigated recently. As one of the most prospective fine-tuning techniques, prompt tuning is proposed to efficiently adapt foundation models to downstream tasks by introducing learnable prompts while freezing the backbones [3, 15, 29, 36, 57, 59, 66, 72, 73]. The learned prompts interweave pre-trained features via the attention mechanism in the vision or language branch, enforcing task-specific distribution shifting.

Despite the improved performance on categories and tasks of interest, recent studies [27, 72] reveal that prompt tuning spoils the parameterized knowledge acquired in pre-training. Without appropriate constraints, the inherent cross-modal alignment is sacrificed for overfitting the downstream tasks, causing the loss of model generalization. As shown in Fig. 1, compared with the zero-shot CLIP, the fine-tuned CLIP by CoOp [73] experiences a performance reduction by 11% on unseen classes across 11 distinct datasets. Therefore, it is of great importance to simultaneously enhance downstream performance and maintain strong generalizability after prompt tuning. Existing studies proposed implicit or explicit regularization to better preserve the general knowledge via various techniques like early stopping, data augmentation [12, 30, 42, 74], gradient and prompt constraints [27, 72]. However, these methods fail to systematically analyze the fundamental reasons behind such model degeneration after prompt tuning.

In this paper, we provide a pioneering explanation of the underlying reasons behind the degradation of model generalization. We propose the **feature shift** as a tool to quantify the inter-modal discrepancy of representations, and thereafter discover the relationship between such discrepancy and model generalization. The newly incorporated learnable prompts, either present in vision or language branches, contribute to the cumulative feature shifts layer-by-layer. Consequently, asynchronous changes occur independently over features of the image and text modalities under the data-scarce scenarios of downstream fine-tuning. We primarily address such inter-modal inconsistency and propose **RESTORE**: **towaRds fEature ShifT for visiOn-language pRrompt lEarning**. Specifically, we design a cross-modal constraint on feature shift, which minimizes the measured distance between the visual and textual feature shifts to impose constraints on the synchrony of image and text encoders for alignment. In order to prevent the prompt-intervened features severely deviating from the pre-trained features simultaneously for both vision and language modalities, we further develop a "surgery" block to act upon the output features for mitigation of misalignment. Such blocks, implemented as adapters, are respectively governed by the extent of visual and textual feature shift and thereby correct representations dynamically.

Our main contribution can be summarized as follows:

1. We systematically and quantitatively explain the reason, namely feature shift, behind the degraded generalizability of VLMs during prompt tuning.
2. We propose the feature shift consistency loss from the perspective of cross-modal alignment to minimize the discrepancy between the two modalities.
3. We propose the "surgery" block to counteract potential severe feature shifts to avoid overfitting and ensure alignment on output representations.
4. Extensive experiments of few-shot prompt tuning on 11 datasets confirm the superiority and validity of our feature shift loss and "surgery" block over state-of-the-art (SOTA) methods.

2 Related Work

2.1 Vision-Language Model

Recently, VLMs [43] [23] [67] [60] [64] [14] [13] have showcased remarkable achievements across a broad range of tasks. The high transferability of pre-trained VLMs has been validated on downstream tasks such as few-shot and zero-shot image recognition [11] [73], cross-modal generation [38] [41] [44] and vision question answering [71] [21]. The VLM pre-training is usually guided by certain vision-language objectives [60] [62] that enable models to learn image-text correspondences from the large-scale image-text pairs [47] [68]. Nonetheless, effectively applying VLMs to downstream tasks remains a complex issue. A typical model is CLIP [43], which utilizes vision-language contrastive learning for informative vision-language representation. In the present study, we choose CLIP as our testbed due to its wide usability and comparability.

2.2 Multi-Modal Prompt Tuning for VLMs

Prompt tuning is first proposed in NLP to effectively fine-tune the large-scale model with the backbone frozen [31] [29]. The instructions in the form of a fixed sentence template are usually given to the language model (known as language prompt), allowing it to better understand the task. CoOp [73] proposed to replace the completely fixed template with a learnable prompt. Co-CoOp [72] added conditioning prompts on image instances to avoid overfitting to certain tasks. Since both vision and language inputs are unified into the same structure under the transformer framework, similar to language prompt tuning, vision prompt also introduces a small number of learnable parameters into the input space while freezing the entire pre-trained transformer backbone during downstream training [24] [22] [57] [5]. Multi-modal prompt tuning [66] [26] [53] [48] [52] [59] [61] [56] [2] is an emerging task that facilitates the simultaneous learning of textual and visual prompts in VLMs. Instead of independently optimizing uni-modal prompts, such a joint-tuning approach encourages interactions between the two modalities during training, leading to adaptable alignments. Several studies proposed to enhance the generalization on downstream tasks by remaining knowledge inheritance and reduce the forgetting of the origin CLIP model [59] [63] [27] [65]. Other methods [69] [70] improve the downstream few-shot performance by adapting the output logits of VLMs.

2.3 Adapters

Adapters were first proposed as lightweight modules in the field of natural language processing [50] [19] for efficient model adaptation. With the development of the vision-language model like CLIP [43], a large number of CLIP-based adapters have been proposed [11] [69] [32] [51] to allow pre-trained models to better transfer to downstream tasks by inserting new learnable lightweight modules [6] [33] [34] [4]. These adapters enhance adaptation by either incorporating prior knowledge into the model or optimizing output representations of existing models. In this paper, we propose the "surgery" block, which is controlled by the feature shift to better alleviate the representation misalignment.

3 Methodology

The proposed method aims to enhance the generalization capabilities of a pre-trained CLIP model for downstream tasks through multi-modal prompt tuning. We start by introducing the process of contrastive language-image pre-training and task-specific fine-tuning, highlighting the intrinsic limitations of single-modal prompt tuning. Subsequently, as illustrated in Fig. 2, we explain the mechanism of multi-modal prompt tuning. Then, the concept of feature shift is proposed, followed by the definition of inter-modal discrepancy in feature shifts and its relationship with model generalization. The cross-modal consistency is achieved by minimizing such inter-modal discrepancy. Finally, we present details about the implementation of "surgery" blocks, especially around their control by feature shift to effectively address the deviated features.

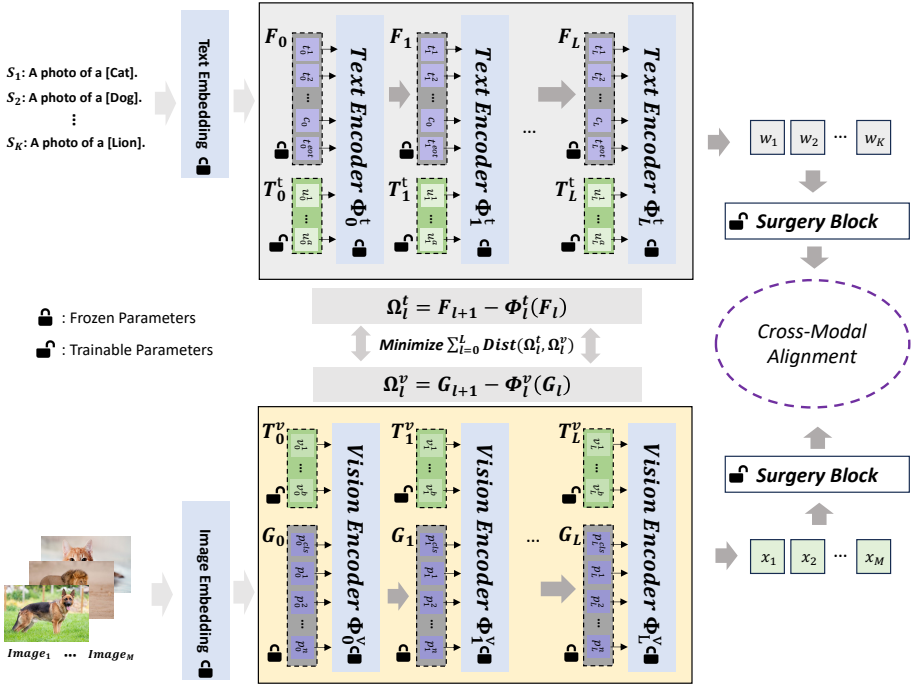


Fig. 2: The overall workflow of our multi-modal prompt tuning. During fine-tuning, we fix the parameters of the encoder backbones unchanged. K different textual descriptions are prompted to represent K categories and are encoded by the text encoder into the embedding space. Similarly, M images are encoded by the image encoder into the visual embedding space. The classification is carried out by measuring the similarity between visual and textual representations. In both vision and language encoders, multiple learnable prompts are equipped to interfere with the embeddings independently. To establish connections between prompts from different modalities, we take feature shift as a bridge and synchronize the cross-modal representation update. In consideration of the risk of task-specific overfitting, the "surgery" block is applied to effectively penalize severe deviation of prompt-tuned features from their pre-trained counterparts, preserving the valuable intrinsic knowledge.

3.1 Contrastive Vision Language Pre-training

In the vision language pre-training framework, positive samples are pairs of images and their corresponding texts, while mismatched images and texts serve as negative samples. Through the contrastive learning of positive and negative sample pairs, vision language models obtain strong generalization ability. During the inference stages, a manually designed prompt is incorporated into the textual component to create a zero-shot linear classifier. This involves encoding class names present in the target dataset into embeddings. For instance, in the classification task, the "[CLASS]" token is first expanded into a prompt

using a predefined template, such as "a photo of a [CLASS]." Subsequently, the filled prompt is embedded by the text encoder into the embedding space as $F^i = \{\mathbf{t}^1, \mathbf{t}^2, \dots, \mathbf{t}^m, \mathbf{c}^i, \mathbf{t}^{eot}\}$, $i \in [1, K]$, where K is the total category number. Here \mathbf{c}^i is the class token and \mathbf{t}^{eot} is the end token of the sequence. Simultaneously, visual features are represented as $G = \{\mathbf{p}^{cls}, \mathbf{p}^1, \dots, \mathbf{p}^n\}$. We denote the language and vision encoders as f and g respectively. The latent text feature for i_{th} category is defined as $\mathbf{w}_i = f(F^i)$. Similarly, the latent image feature is defined as $\mathbf{x} = g(G)$. The class prediction probability y can be computed as follows:

$$p(y = i) = \frac{\exp(\text{sim}(\mathbf{x}, \mathbf{w}_i) / \tau)}{\sum_{j=1}^K \exp(\text{sim}(\mathbf{x}, \mathbf{w}_j) / \tau)}, \quad (1)$$

where $\text{sim}(\cdot, \cdot)$ represents cosine similarity, and τ is the temperature coefficient.

3.2 Multi-Modal Prompt Tuning

Prompt tuning methods fine-tune the model by introducing learnable prompts. We denote $\mathbf{T}_l^v = \{\mathbf{v}_l^1, \mathbf{v}_l^2, \dots, \mathbf{v}_l^a\}$ and $\mathbf{T}_l^t = \{\mathbf{u}_l^1, \mathbf{u}_l^2, \dots, \mathbf{u}_l^b\}$ respectively as learnable vision and text prompts of the l_{th} transformer block, where a and b represent the number of tokens that can be learned. The vision embedding is defined as the concatenation of learnable prompts and frozen image embeddings: $[\mathbf{T}_l^v, \mathbf{G}_l]$. The text embedding is defined as the concatenation of text prompts and class embeddings: $[\mathbf{T}_l^t, \mathbf{F}_l]$. Out of simplicity, we present the formulation of vision prompt tuning as a demonstration and that of text prompt tuning can be derived similarly. The vanilla vision prompt tuning can be realized by interfering with visual features at each layer (the embeddings marked red are learnable):

$$\begin{aligned} [\mathbf{T}_1^v, \mathbf{G}_1] &= \Phi_0([\mathbf{T}_0^v, \mathbf{G}_0]), \\ [\mathbf{T}_l^v, \mathbf{G}_l] &= \Phi_{l-1}([\mathbf{T}_{l-1}^v, \mathbf{G}_{l-1}]), l = 2, 3, \dots, L, \end{aligned} \quad (2)$$

In this work, we follow the deep prompt tuning paradigm, where we introduce independent learnable prompts for each layer as follows:

$$[_, \mathbf{G}_l] = \Phi_{l-1}([\mathbf{T}_{l-1}^v, \mathbf{G}_{l-1}]), l = 1, 2, \dots, L. \quad (3)$$

Therefore, the image feature $\tilde{\mathbf{x}}$ and text feature $\tilde{\mathbf{w}}_i$ of i_{th} class can be obtained by $g(G, \{T_l^v\}_{l=1}^L)$ and $f(F^i, \{T_l^t\}_{l=1}^L)$, then the prediction can be calculated as follows:

$$p(y = i) = \frac{\exp(\text{sim}(\tilde{\mathbf{x}}, \tilde{\mathbf{w}}_i))}{\sum_{j=1}^K \exp(\text{sim}(\tilde{\mathbf{x}}, \tilde{\mathbf{w}}_j))}. \quad (4)$$

Given the one-hot label of the images \hat{y} , we use cross-entropy \mathcal{L}^{ce} as our final training loss:

$$\mathcal{L}^{ce} = -CrossEntropy(\hat{y}, y) \quad (5)$$

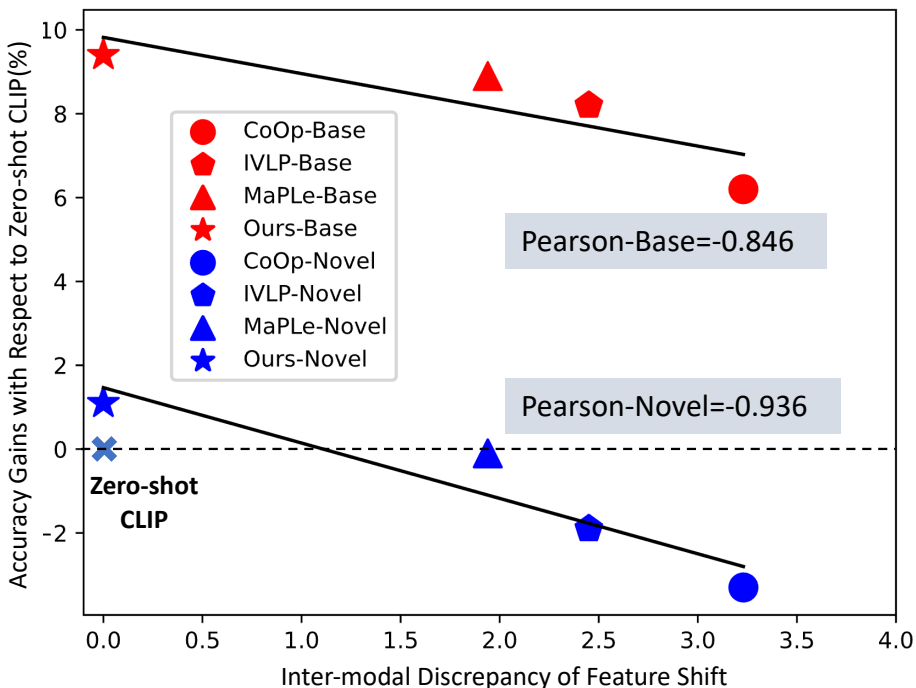


Fig. 3: The negatively associated relationship is observed between the inter-modal discrepancy of feature shift and the performance gains. Compared with the zero-shot CLIP, existing single-modal and multi-modal prompt tuning methods achieve superior and inferior performance respectively on base and novel categories. They "unintentionally" encourage the inter-modal discrepancy of feature shift during fine-tuning, consequently leading to a loss of generalization capabilities for downstream tasks.

3.3 Feature Shift in Multi-Modal Prompt Tuning

Feature Shift. It is of great importance to impose proper constraints during prompt tuning for: 1) mitigating the issue of model collapse and 2) improving the efficiency of knowledge transfer for novel visual and textual concepts [27, 30, 35, 58, 74]. Various strategies have been put forth in the literature [25, 27, 74], with the primary aim of avoiding overfitting and model collapse. Nonetheless, none of these studies has paid enough attention to the underlying causes of model collapse in multi-modal systems. Our assumption is that, the pre-trained CLIP enjoys a high level of generalization over various downstream tasks thanks to its highly aligned cross-modal representations. The degradation of such alignment, which takes place in overfitting images or texts of specific domains or formats, can be ascribed to the asynchronous, inconsistent updates of visual and textual features. Such inter-modal discrepancy of features should be quantified for analysis of model generalization. We first propose the concept of **feature shift**, which is used to estimate the variation of features generated

by the vision-language model caused by the prompt tuning. **Specifically, we define feature shift as the difference in feature representations of images or texts by transformer block with/without the introduction of learnable parameters.** For the l_{th} vision/text transformer block Φ_l^v/Φ_l^t , given its corresponding inputs feature G_l/F_l and learnable parameters T_l^v/T_l^t , the feature shift Ω_l^v and Ω_l^t are respectively defined as:

$$\begin{aligned}\Omega_l^v &= \mathbf{G}_{l+1} - \Phi_l^v(\mathbf{G}_l), & [_, \mathbf{G}_{l+1}] &= \Phi_l^v([\mathbf{T}_l^v, \mathbf{G}_l]), \\ \Omega_l^t &= \mathbf{F}_{l+1} - \Phi_l^t(\mathbf{F}_l), & [_, \mathbf{F}_{l+1}] &= \Phi_l^t([\mathbf{T}_l^t, \mathbf{F}_l]).\end{aligned}\quad (6)$$

Inter-modal Discrepancy of Feature Shift. We propose the feature shift as an explanatory tool to decipher such seesaw performance of prompt tuning methods (CoOp [73], IVLP [27, 45], and MaPLe [26]) on base and novel classes. By observing the inter-modal discrepancy of feature shift versus the performance gains (see Fig. 3), we can intuitively see the correlation that with larger feature shift variation, the model tends to perform worse. Therefore, in Sec. 3.4, we propose feature shift consistency loss for cross-modal alignment.

3.4 Feature Shift Consistency for Cross Modality Alignment

Our intuition is that model misalignment is not only attributable to the deviation in either the visual or textual from the original CLIP embedding space. Moreover, it stems from inconsistent feature shifts on both branches. To enhance the cross-modal alignment, the discrepancies caused by the introduced prompts in different modality branches should be minimized. In practice, we try to minimize the distance of these feature shifts between different modalities in the feature space. For the vision encoder and language encoder, given the feature shift on both vision and language branches as Ω_l^v and Ω_l^t , the feature shift loss of the l_{th} transformer block is defined as follows:

$$\mathbf{L}_l^{\text{fs}} = \text{Dist}(\Omega_l^v, \Omega_l^t) \quad (7)$$

where **Dist** represents a measurement of the distance between feature variations of different modalities. Here we employ the mean square error between the matrix norm, and the final loss is defined as follows:

$$\mathbf{L}_l^{\text{fs}} = \text{MSE}(\text{Norm}(\Omega_l^v) - \text{Norm}(\Omega_l^t)) \quad (8)$$

where **Norm** represents the Frobenius norm. For the feature shift of different transformer blocks, we use a hierarchical alignment strategy, and the full loss expression is defined as follows:

$$\mathcal{L}^{\text{fs}} = \sum_{l=1}^L \mathbf{L}_l^{\text{fs}} \quad (9)$$

The overall loss function is the weighted summary of cross-entropy loss \mathcal{L}^{ce} and the feature shift loss \mathcal{L}^{fs} with weight coefficient λ_{f_s} as follows:

$$\mathcal{L}_{\text{total}} = \lambda_{f_s} \mathcal{L}^{\text{fs}} + \mathcal{L}^{\text{ce}} \quad (10)$$

3.5 Surgery Block with Feature Shift Guidance

One potential hacking way that bypasses the proposed cross-modal alignment constraint is to concurrently promote large feature shifts for both prompt-tuned visual and textual features, where the layer-wise inter-modal discrepancy is estimated small but the overall accumulated deviation from pre-trained features can be huge. The relative difference between feature shifts of two modalities can still be small (see Eq. 9) if their Frobenius norm evolves with the same trend and at the same pace. Consequently, the model is still prone to task-specific overfitting. In this case, we propose the surgery block acting on both the two modalities in order to dynamically penalize cross-modal misalignment. The operation of this surgery block is governed by the measured scale of feature shift, meaning that a stronger correction effect is to be expected if a larger feature shift is detected. As depicted in Fig. 2, the surgery block is implemented as an adapter as follows:

$$\begin{aligned}
 \tilde{\mathbf{x}} &= \alpha_v * \text{Surgery}(\tilde{\mathbf{x}}) + \tilde{\mathbf{x}}, \\
 \tilde{\mathbf{w}}_i &= \alpha_t * \text{Surgery}(\tilde{\mathbf{w}}_i) + \tilde{\mathbf{w}}_i, \\
 \alpha_v &= \gamma \sum_{l=1}^L \text{Norm}(\Omega_l^v), \\
 \alpha_t &= \beta \sum_{l=1}^L \text{Norm}(\Omega_l^t), \\
 \text{Surgery}(\tilde{\mathbf{x}}) &= \text{ReLU}(LN(\tilde{\mathbf{x}}) \cdot \mathbf{W}_{\text{up}}) \cdot \mathbf{W}_{\text{down}},
 \end{aligned} \tag{11}$$

where γ, β are hyper-parameters. \mathbf{W}_{up} and \mathbf{W}_{down} represent up-scale and down-scale linear mappings, respectively. LN represents the layer normalization. We dynamically update α_v and α_t to control the surgery during training.

4 Experiments

4.1 Datasets and Implementation Details

Datasets. Following previous prompt tuning studies, we validate our method on 11 few-shot classification datasets, including ImageNet [8], StanfordCars [28], UCF101 [49], Caltech101 [10], Flowers102 [39], SUN397 [55], DTD [7], EuroSAT [16], FGVCaircraft [37], OxfordPets [40] and Food101 [1]. OxfordPets, Food101, StanfordCars, Flowers102, and FGVCaircraft belong to fine-grained classification tasks, EuroSAT is for remote sensing classification, and DTD is the dataset of texture classification. The partitioning of all datasets follows [72] [73].

Implementation Details. We adopt a few-shot training strategy in all experiments at 16 shots which are randomly sampled for each class. We apply our multi-modal prompt tuning method on a pre-trained CLIP model with ViT-B/16 [9] as the image encoder. Each model is trained with a batch size of 4 and a learning rate of 0.0035 via SGD optimizer on a single NVIDIA RTX3090 GPU. For cross-dataset evaluation and cross-domain evaluation, each model is trained

for 4 epochs due to computing resources constraint while in base-to-novel evaluation the training epochs is 10. Besides, we report the results over 3 different random seeds to make results reliable. For a fair comparison, the text description of each class is simply initialized as "a photo of a [CLASS]" for each method.

4.2 Base-to-Novel Evaluation

We first follow [26] to evaluate our method under the base-to-novel setting, where we evenly divide datasets into two groups: the base classes and the novel classes. The model undergoes training on the base classes and is subsequently assessed on its performance with respect to both the base and unseen novel classes. This benchmark serves as a means to gauge the model’s generalization capability.

Table 1 presents the comparison between the proposed method and baselines including Zero-shot CLIP, CoOp [73], Co-CoOp [72], MaPLe [26], Prompt-SRC [27] on 11 datasets. Our approach directly imposes stronger alignment constraints on different modality branches hierarchically, and introduces the surgery for the output feature to alleviate the misalignment problem. This not only improves the performance on the base class but also improves the performance on the unseen class clearly.

4.3 Cross Dataset/Domain Evaluation

To further validate the generalization ability of our method, we tuned our model on ImageNet and tested on other datasets. Under the cross-dataset setting, each model is tested on the other ten target datasets, while under the cross-domain setting, we assess the performance on several variants of ImageNet: ImageNetV2 [46], ImageNet-Sketch [54], ImageNet-A [18], and ImageNet-R [17]. As depicted in Table 2 and 3, our method surpasses other approaches on the majority of the datasets, demonstrating its ability to maintain an exceptional level of generalization even in situations with significant domain gaps.

4.4 Ablation

In this section we explore the effectiveness of the various modules that have been proposed modules.

Effectiveness of Feature Shift Loss. We conducted an investigation into the impact of the feature shift loss. By adjusting the coefficients of the loss, we compared the performance changes of the base and novel classes on different datasets. Table 4 presents that as the coefficient increases, the performance on the base class decreases while the performance on the novel class increases. This observation demonstrates that the feature shift loss, which aligns modalities, effectively maintains and improves the alignment ability of the vision-language model. Taking into account the results for both the base and novel classes, we set the coefficient λ_{fs} to 1.

Effectiveness of FS-Guided Surgery Block. As shown in Table 5, our surgery block offers greater advantages for the new class rather than the base

Table 1: Base-to-Novel evaluation. We uniformly chose the same epoch number (10 epochs) for the fairness of comparison. We reproduce the results of prompt tuning methods and build our method on the basis of MaPLe and PromptSRC methods, with **RESTORE_m** implemented based on MaPLe and **RESTORE_p** based on PromptSRC. HM is the harmonic mean of classification accuracy on base class and novel class.

(a) Average on 11 datasets

Method	Base Novel	HM
<i>Zero-shot</i>		
CLIP	69.34 74.22	71.70
<i>Prompt Tuning</i>		
CoOp	81.84 70.94	76.00
Co-CoOp	79.38 73.11	76.11
MaPLe	83.47 74.09	78.50
RESTORE_m	83.93 75.60	79.55(+1.1)
PromptSRC	83.14 75.11	78.92
RESTORE_p	83.44 76.35	79.74(+0.8)

(b) ImageNet

Method	Base Novel	HM
<i>Zero-shot</i>		
CLIP	72.43 68.14	70.22
<i>Prompt Tuning</i>		
CoOp	76.67 69.73	73.03
Co-CoOp	75.99 70.77	73.28
MaPLe	77.11 69.49	73.10
RESTORE_m	77.42 69.83	73.43(+0.3)
PromptSRC	77.30 70.66	73.83
RESTORE_p	77.39 70.88	73.99(+0.2)

(c) Caltech101

Method	Base Novel	HM
<i>Zero-shot</i>		
CLIP	96.84 94.00	95.40
<i>Prompt Tuning</i>		
CoOp	97.94 94.32	96.09
Co-CoOp	97.72 93.08	95.34
MaPLe	98.41 95.05	96.70
RESTORE_m	98.30 95.61	96.94(+0.2)
PromptSRC	97.83 94.25	96.00
RESTORE_p	97.84 94.84	96.32(+0.3)

(d) OxfordPets

Method	Base Novel	HM
<i>Zero-shot</i>		
CLIP	91.17 97.26	94.12
<i>Prompt Tuning</i>		
CoOp	95.55 97.43	96.48
Co-CoOp	94.84 97.60	96.20
MaPLe	95.16 97.78	96.45
RESTORE_m	95.59 98.03	96.79(+0.3)
PromptSRC	95.50 97.16	96.32
RESTORE_p	95.56 98.04	96.78(+0.4)

(e) StanfordCars

Method	Base Novel	HM
<i>Zero-shot</i>		
CLIP	63.37 74.89	68.65
<i>Prompt Tuning</i>		
CoOp	74.49 70.87	72.63
Co-CoOp	69.87 74.69	72.20
MaPLe	76.22 73.08	74.62
RESTORE_m	78.10 73.29	75.61(+1.0)
PromptSRC	76.04 75.41	75.72
RESTORE_p	76.61 76.01	76.31(+0.6)

(f) Flowers102

Method	Base Novel	HM
<i>Zero-shot</i>		
CLIP	72.08 77.80	74.83
<i>Prompt Tuning</i>		
CoOp	96.96 72.41	82.89
Co-CoOp	93.00 72.84	81.69
MaPLe	96.99 73.59	83.69
RESTORE_m	97.66 74.30	84.39(+0.7)
PromptSRC	97.69 76.53	85.82
RESTORE_p	97.63 76.74	85.93(+0.1)

(g) Food101

Method	Base Novel	HM
<i>Zero-shot</i>		
CLIP	90.10 91.22	90.66
<i>Prompt Tuning</i>		
CoOp	90.32 91.23	90.77
Co-CoOp	90.68 91.71	91.19
MaPLe	90.07 91.54	90.80
RESTORE_m	90.46 91.74	91.10(+0.3)
PromptSRC	90.69 91.74	91.21
RESTORE_p	90.82 91.75	91.28(+0.1)

(h) FGVC Aircraft

Method	Base Novel	HM
<i>Zero-shot</i>		
CLIP	72.43 68.14	70.22
<i>Prompt Tuning</i>		
CoOp	37.98 32.35	34.93
Co-CoOp	36.09 34.21	35.12
MaPLe	39.88 34.03	36.70
RESTORE_m	40.62 36.37	38.36(+1.7)
PromptSRC	37.66 28.27	31.27
RESTORE_p	39.58 36.85	38.17(+6.9)

(i) SUN397

Method	Base Novel	HM
<i>Zero-shot</i>		
CLIP	69.36 75.35	72.23
<i>Prompt Tuning</i>		
CoOp	80.83 75.30	77.96
Co-CoOp	79.27 76.84	78.03
MaPLe	81.68 77.58	79.57
RESTORE_m	81.97 77.31	79.57(+0.0)
PromptSRC	82.44 78.75	80.55
RESTORE_p	82.52 78.88	80.66(+0.1)

(j) DTD

Method	Base Novel	HM
<i>Zero-shot</i>		
CLIP	53.24 59.90	56.37
<i>Prompt Tuning</i>		
CoOp	78.90 48.35	59.78
Co-CoOp	73.80 56.04	63.70
MaPLe	81.36 59.02	68.40
RESTORE_m	82.79 61.83	70.79(+2.4)
PromptSRC	82.67 60.99	70.18
RESTORE_p	82.69 61.64	70.63(+0.4)

(k) EuroSAT

Method	Base Novel	HM
<i>Zero-shot</i>		
CLIP	56.48 64.05	60.03
<i>Prompt Tuning</i>		
CoOp	86.94 56.14	67.91
Co-CoOp	80.94 63.98	71.29
MaPLe	95.73 67.59	79.07
RESTORE_m	94.71 75.97	84.04(+5.0)
PromptSRC	90.69 73.86	81.37
RESTORE_p	91.50 74.45	81.79(+0.4)

(l) UCF101

Method	Base Novel	HM
<i>Zero-shot</i>		
CLIP	70.53 77.50	73.85
<i>Prompt Tuning</i>		
CoOp	83.63 72.20	77.50
Co-CoOp	80.94 72.45	76.46
MaPLe	85.51 76.24	80.60
RESTORE_m	85.66 77.37	81.31(+0.7)
PromptSRC	86.02 78.58	82.13
RESTORE_p	85.95 79.77	82.75(+0.6)

Table 2: Cross dataset evaluation. The model is trained on ImageNet and tested on 10 unseen target datasets. This experiment mainly evaluates the generalization ability of the model between different datasets.

Domain	Dataset	Coop	Co-CoOp	MaPLe	RESTORE _m	PromptSRC	RESTORE _p
Source	ImageNet	70.61%	70.45%	70.78%	71.43% (+0.7)	71.34%	71.55% (+0.2)
Target	Caltech101	93.87%	93.27%	93.35%	93.39%	93.26%	93.69%
	OxfordPets	90.13%	90.68%	89.92%	90.35%	90.21%	90.95%
	StanfordCars	65.70%	65.71%	65.91%	66.46%	65.70%	66.96%
	Flowers102	71.21%	72.35%	71.01%	71.90%	70.25%	71.95%
	Food101	86.13%	86.10%	86.40%	86.55%	86.15%	87.43%
	FGVCaircraft	22.47%	22.11%	24.81%	24.97%	24.14%	23.93%
	SUN397	66.73%	66.71%	66.23%	67.69%	67.09%	68.29%
	DTD	44.64%	47.04%	45.27%	47.10%	46.44%	45.21%
	EuroSAT	44.56%	44.28%	42.80%	45.00%	44.34%	49.34%
	UCF101	67.38%	67.33%	66.69%	67.78%	68.21%	68.21%
Average	65.28%	65.56%	65.24%	66.12% (+0.9)	65.58%	66.60% (+1.0)	

Table 3: Cross domain validation on 4 datasets. Models are trained on ImageNet and tested on several datasets with certain domain gaps.

Domain	Dataset	Coop	Co-CoOp	MaPLe	RESTORE _m	PromptSRC	RESTORE _p
Source	ImageNet	70.61%	70.45%	70.78%	71.43% (+0.7)	71.34%	71.55% (+0.2)
Target	ImageNetV2	63.94%	63.83%	64.14%	64.16%	64.32%	64.67%
	ImageNet-S	49.05%	48.81%	48.82%	49.11%	49.37%	49.93%
	ImageNet-A	51.03%	50.88%	50.16%	50.51%	51.23%	51.45%
	ImageNet-R	77.00%	76.98%	76.75%	77.17%	77.88%	77.64%
Average	60.26%	60.33%	59.97%	60.24% (+0.3)	60.70%	60.92% (+0.2)	

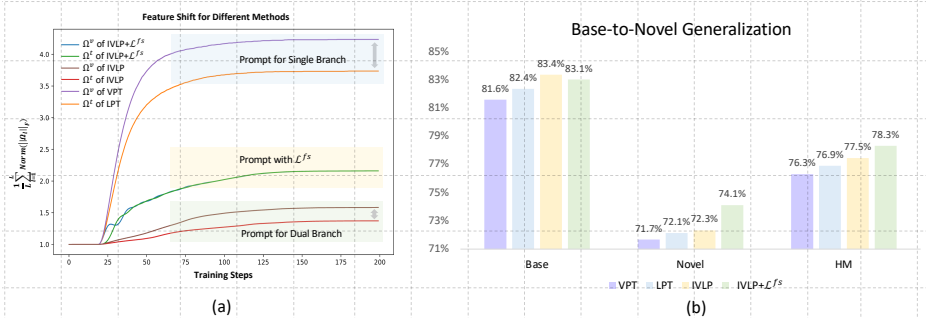


Fig. 4: Average feature shift and the according performance for different methods. IVLP, VPT, LPT, and IVLP+ \mathcal{L}^{fs} represent independent vision-language prompt tuning, vision prompt tuning, language prompt tuning, and IVLP with feature shift loss. The introduction of prompt tuning in a single branch causes severe feature shifts, leading to final feature misalignment and degradation of performance. However, the introduction of our feature shift loss can reduce such kind of modality misalignment, therefore causing superior performance.

class. This can be attributed to the adapter’s precise adaptation of the final embedding, leading to improved generalization. Additionally, we compared adapters

on the language branch, and unrelated prompts on both the visual and language branch to the CLIP model during the fine-tuning process, and compare the feature shift as well as the final model performance. As shown in Fig. 4 (a), we find that the feature shift generated by using only vision prompt or language prompt is larger. This is because there are fewer learnable parameters, so the features of a single modality need to change more to adapt to downstream tasks, which can easily cause overfitting. Due to the introduction of more parameters, the value of the feature shift of IVLP is relatively small, but its variation still exists, which poses a challenge to the alignment ability of models. After the addition of feature shift loss, although the shift of the model will increase, its variation will decrease and its generalization ability will be stronger. From Fig. 4 (b) it is evident that the generalization performance of the model is subpar when using solely vision-side prompts or text-side prompts compared to when both types are combined. After adding \mathcal{L}^{fs} , we find that the performance of the model is further improved, which proves the effectiveness of our feature shift loss.

T-SNE Visualization. We conducted t-SNE visualization (refer to Fig. 5) on features generated by various methods. Our observations revealed that the zero-shot CLIP model displayed subpar performance in the base class, while the CoOp model (vanilla prompt tuning) exhibited limited generalization in the novel class. Conversely, our proposed approach outperformed both the base and novel classes, showcasing superior results.

6 Conclusion

We investigate the reasons behind the degradation of generalization for prompt tuning of vision-language models. We find that cross-modal misalignment can be quantified with our proposed feature shift. The inter-modal discrepancy of feature shift is negatively associated with performance gains on both base and novel classes in downstream tasks. Therefore, we propose RESTORE to adapt prompts in various modalities via the feature shift consistency loss. Additionally, we propose the "surgery" block, a feature-shift guided adapter, to tackle the potential hacking risk out of overfitting. Such adapters effectively adjust representations that undergo large-scale feature shifts. Extensive experiments demonstrate that our method surpasses SOTA methods under multiple evaluation settings.

There are mainly two drawbacks associated with the proposed method. First, it might not be accurate enough to use the mean squared error (MSE) and the Frobenius norm for measuring the discrepancy between feature shifts from different modalities. Alternative distance or divergence measures might be more constructive in capturing such discrepancy. Second, the exploration of prompt tuning might be more focused on engineering and proper theoretical analysis of the relationship between the degenerated model and biased prompts is still lacking. In our future work, we plan to 1) propose evaluation tools of overfitting for prompt tuning with theoretical support, and 2) validate the proposed method on models with larger sizes and generative multi-modal models.

References

1. Bossard, L., Guillaumin, M., Van Gool, L.: Food-101—mining discriminative components with random forests. In: ECCV. pp. 446–461. Springer (2014) [9](#)
2. Cao, G., Shi, K., Fu, H., Zhang, H., Xu, G.: Aple: Token-wise adaptive for multi-modal prompt learning. arXiv preprint arXiv:2401.06827 (2024) [4](#)
3. Chen, G., et al.: Prompt learning with optimal transport for vision-language models. arXiv preprint arXiv:2210.01253 (2022) [2](#)
4. Chen, S., et al.: Adaptformer: Adapting vision transformers for scalable visual recognition. *Advances in Neural Information Processing Systems* **35**, 16664–16678 (2022) [4](#)
5. Chen, W., et al.: Semantic prompt for few-shot image recognition. In: CVPR. pp. 23581–23591 (2023) [4](#)
6. Chen, Z., et al.: Vision transformer adapter for dense predictions. arXiv preprint arXiv:2205.08534 (2022) [4](#)
7. Cimpoi, M., Maji, S., Kokkinos, I., Mohamed, S., Vedaldi, A.: Describing textures in the wild. In: CVPR. pp. 3606–3613 (2014) [9](#)
8. Deng, J., Dong, W., Socher, R., Li, L.J., Li, K., Fei-Fei, L.: Imagenet: A large-scale hierarchical image database. In: CVPR. pp. 248–255. Ieee (2009) [9](#)
9. Dosovitskiy, A., Beyer, L., Kolesnikov, A., Weissenborn, D., Zhai, X., Unterthiner, T., Dehghani, M., Minderer, M., Heigold, G., Gelly, S., et al.: An image is worth 16x16 words: Transformers for image recognition at scale. arXiv preprint arXiv:2010.11929 (2020) [9](#)
10. Fei-Fei, L., Fergus, R., Perona, P.: Learning generative visual models from few training examples: An incremental bayesian approach tested on 101 object categories. In: CVPRW. pp. 178–178. IEEE (2004) [9](#)
11. Gao, P., et al.: Clip-adapter: Better vision-language models with feature adapters. *IJCV* pp. 1–15 (2023) [3](#), [4](#)
12. Gao, T., et al.: Making pre-trained language models better few-shot learners. arXiv preprint arXiv:2012.15723 (2020) [2](#)
13. Gao, Y., Liu, J., Xu, Z., Wu, T., Liu, W., Yang, J., Li, K., Sun, X.: Softclip: Softer cross-modal alignment makes clip stronger. arXiv preprint arXiv:2303.17561 (2023) [3](#)
14. Gao, Y., Liu, J., Xu, Z., Zhang, J., Li, K., Ji, R., Shen, C.: Pyramidclip: Hierarchical feature alignment for vision-language model pretraining. *Advances in neural information processing systems* **35**, 35959–35970 (2022) [3](#)
15. Guo, Z., et al.: Texts as images in prompt tuning for multi-label image recognition. In: CVPR. pp. 2808–2817 (2023) [2](#)
16. Helber, P., Bischke, B., Dengel, A., Borth, D.: Eurosat: A novel dataset and deep learning benchmark for land use and land cover classification. *IEEE Journal of Selected Topics in Applied Earth Observations and Remote Sensing* **12**(7), 2217–2226 (2019) [9](#)
17. Hendrycks, D., et al.: The many faces of robustness: A critical analysis of out-of-distribution generalization. In: ICCV. pp. 8340–8349 (2021) [10](#)
18. Hendrycks, D., et al.: Natural adversarial examples. In: CVPR. pp. 15262–15271 (2021) [10](#)
19. Housley, N., et al.: Parameter-efficient transfer learning for nlp. In: ICML. pp. 2790–2799. PMLR (2019) [4](#)
20. Hu, E.J., et al.: Lora: Low-rank adaptation of large language models. arXiv preprint arXiv:2106.09685 (2021) [2](#)

21. Hu, Y., et al.: Promptcap: Prompt-guided image captioning for vqa with gpt-3. In: ICCV. pp. 2963–2975 (2023) [3](#)
22. Huang, Q., Dong, X., Chen, D., Zhang, W., Wang, F., Hua, G., Yu, N.: Diversity-aware meta visual prompting. In: CVPR. pp. 10878–10887 (2023) [4](#)
23. Jia, C., et al.: Scaling up visual and vision-language representation learning with noisy text supervision. In: ICML. pp. 4904–4916. PMLR (2021) [1](#), [3](#)
24. Jia, M., Tang, L., Chen, B.C., Cardie, C., Belongie, S., Hariharan, B., Lim, S.N.: Visual prompt tuning. In: ECCV. pp. 709–727. Springer (2022) [2](#), [4](#)
25. Kan, B., Wang, T., Lu, W., Zhen, X., Guan, W., Zheng, F.: Knowledge-aware prompt tuning for generalizable vision-language models. In: ICCV. pp. 15670–15680 (2023) [7](#)
26. Khattak, M.U., Rasheed, H., Maaz, M., Khan, S., Khan, F.S.: Maple: Multi-modal prompt learning. In: CVPR. pp. 19113–19122 (2023) [4](#), [8](#), [10](#)
27. Khattak, M.U., et al.: Self-regulating prompts: Foundational model adaptation without forgetting. In: ICCV. pp. 15190–15200 (2023) [2](#), [4](#), [7](#), [8](#), [10](#)
28. Krause, J., Stark, M., Deng, J., Fei-Fei, L.: 3d object representations for fine-grained categorization. In: ICCVW. pp. 554–561 (2013) [9](#)
29. Lester, B., Al-Rfou, R., Constant, N.: The power of scale for parameter-efficient prompt tuning. arXiv preprint arXiv:2104.08691 (2021) [2](#), [4](#)
30. Li, J., et al.: Gradient-regulated meta-prompt learning for generalizable vision-language models. arXiv preprint arXiv:2303.06571 (2023) [2](#), [7](#)
31. Li, X.L., Liang, P.: Prefix-tuning: Optimizing continuous prompts for generation. arXiv preprint arXiv:2101.00190 (2021) [2](#), [4](#)
32. Li, X., Lian, D., Lu, Z., Bai, J., Chen, Z., Wang, X.: Graphadapter: Tuning vision-language models with dual knowledge graph. arXiv preprint arXiv:2309.13625 (2023) [2](#), [4](#)
33. Li, Y., et al.: Benchmarking detection transfer learning with vision transformers. arXiv preprint arXiv:2111.11429 (2021) [4](#)
34. Li, Y., et al.: Exploring plain vision transformer backbones for object detection. In: European Conference on Computer Vision. pp. 280–296. Springer (2022) [4](#)
35. Li, Z., Hoiem, D.: Learning without forgetting. TPAMI **40**(12), 2935–2947 (2017) [7](#)
36. Liu, X., Zheng, Y., Du, Z., Ding, M., Qian, Y., Yang, Z., Tang, J.: Gpt understands, too. AI Open (2023) [2](#)
37. Maji, S., Rahtu, E., Kannala, J., Blaschko, M., Vedaldi, A.: Fine-grained visual classification of aircraft. arXiv preprint arXiv:1306.5151 (2013) [9](#)
38. Nichol, A., et al.: Glide: Towards photorealistic image generation and editing with text-guided diffusion models. arXiv preprint arXiv:2112.10741 (2021) [3](#)
39. Nilsback, M.E., Zisserman, A.: Automated flower classification over a large number of classes. In: 2008 Sixth Indian conference on computer vision, graphics & image processing. pp. 722–729. IEEE (2008) [9](#)
40. Parkhi, O.M., Vedaldi, A., Zisserman, A., Jawahar, C.: Cats and dogs. In: CVPR. pp. 3498–3505. IEEE (2012) [9](#)
41. Patashnik, O., et al.: Styleclip: Text-driven manipulation of stylegan imagery. In: ICCV. pp. 2085–2094 (2021) [3](#)
42. Qin, C., Joty, S.: Lfpt5: A unified framework for lifelong few-shot language learning based on prompt tuning of t5. arXiv preprint arXiv:2110.07298 (2021) [2](#)
43. Radford, et al.: Learning transferable visual models from natural language supervision. In: ICML. pp. 8748–8763. PMLR (2021) [1](#), [3](#), [4](#)

44. Ramesh, A., Dhariwal, P., Nichol, A., Chu, C., Chen, M.: Hierarchical text-conditional image generation with clip latents, 2022. URL <https://arxiv.org/abs/2204.06125> **7** (2022) **3**
45. Rasheed, H., Khattak, M.U., Maaz, M., Khan, S., Khan, F.S.: Fine-tuned clip models are efficient video learners. In: Proceedings of the IEEE/CVF Conference on Computer Vision and Pattern Recognition. pp. 6545–6554 (2023) **8**
46. Recht, B., Roelofs, R., Schmidt, L., Shankar, V.: Do imagenet classifiers generalize to imagenet? In: ICML. pp. 5389–5400. PMLR (2019) **10**
47. Schuhmann, C., et al.: Laion-5b: An open large-scale dataset for training next generation image-text models. NIPS **35**, 25278–25294 (2022) **3**
48. Shi, C., Yang, S.: Logoprompt: Synthetic text images can be good visual prompts for vision-language models. In: ICCV. pp. 2932–2941 (2023) **4**
49. Soomro, K., Zamir, A.R., Shah, M.: Ucf101: A dataset of 101 human actions classes from videos in the wild. arXiv preprint arXiv:1212.0402 (2012) **9**
50. Stickland, A.C., Murray, I.: Bert and pals: Projected attention layers for efficient adaptation in multi-task learning. In: ICML. pp. 5986–5995. PMLR (2019) **4**
51. Sung, Y.L., Cho, J., Bansal, M.: Vl-adapter: Parameter-efficient transfer learning for vision-and-language tasks. In: CVPR. pp. 5227–5237 (2022) **4**
52. Tu, C.H., Mai, Z., Chao, W.L.: Visual query tuning: Towards effective usage of intermediate representations for parameter and memory efficient transfer learning. In: CVPR. pp. 7725–7735 (2023) **4**
53. Wang, D., Li, M., Liu, X., Xu, M., Chen, B., Zhang, H.: Tuning multi-mode token-level prompt alignment across modalities. arXiv preprint arXiv:2309.13847 (2023) **4**
54. Wang, H., et al.: Learning robust global representations by penalizing local predictive power. NIPS **32** (2019) **10**
55. Xiao, J., Hays, J., Ehinger, K.A., Oliva, A., Torralba, A.: Sun database: Large-scale scene recognition from abbey to zoo. In: 2010 IEEE computer society conference on computer vision and pattern recognition. pp. 3485–3492. IEEE (2010) **9**
56. Xing, Y., et al.: Dual modality prompt tuning for vision-language pre-trained model. IEEE Transactions on Multimedia (2023) **4**
57. Xing, Y.o.: Class-aware visual prompt tuning for vision-language pre-trained model. arXiv preprint arXiv:2208.08340 (2022) **2, 4**
58. Yang, Y., et al.: Pick the best pre-trained model: Towards transferability estimation for medical image segmentation. In: MICCAI. pp. 674–683. Springer (2023) **7**
59. Yao, H., et al.: Visual-language prompt tuning with knowledge-guided context optimization. In: CVPR. pp. 6757–6767 (2023) **2, 4**
60. Yao, L., et al.: Filip: Fine-grained interactive language-image pre-training. arXiv preprint arXiv:2111.07783 (2021) **3**
61. Yao, Y., Zhang, A., Zhang, Z., Liu, Z., Chua, T.S., Sun, M.: Cpt: Colorful prompt tuning for pre-trained vision-language models. arXiv preprint arXiv:2109.11797 (2021) **4**
62. Yu, J., et al.: Coca: Contrastive captioners are image-text foundation models. arXiv preprint arXiv:2205.01917 (2022) **3**
63. Yu, T., Lu, Z., Jin, X., Chen, Z., Wang, X.: Task residual for tuning vision-language models. In: CVPR. pp. 10899–10909 (2023) **4**
64. Yuan, L., et al.: Florence: A new foundation model for computer vision. arXiv preprint arXiv:2111.11432 (2021) **3**
65. Zang, Y., Goh, H., Susskind, J., Huang, C.: Overcoming the pitfalls of vision-language model finetuning for ood generalization. arXiv preprint arXiv:2401.15914 (2024) **4**

66. Zang, Y., et al.: Unified vision and language prompt learning. arXiv preprint arXiv:2210.07225 (2022) [2](#), [4](#)
67. Zhai, X., et al.: Lit: Zero-shot transfer with locked-image text tuning. In: CVPR. pp. 18123–18133 (2022) [3](#)
68. Zhang, J., Huang, J., Jin, S., Lu, S.: Vision-language models for vision tasks: A survey. arXiv preprint arXiv:2304.00685 (2023) [3](#)
69. Zhang, R., Fang, R., Zhang, W., Gao, P., Li, K., Dai, J., Qiao, Y., Li, H.: Tip-adapter: Training-free clip-adapter for better vision-language modeling. arXiv preprint arXiv:2111.03930 (2021) [2](#), [4](#)
70. Zhang, R., et al.: Prompt, generate, then cache: Cascade of foundation models makes strong few-shot learners. In: CVPR. pp. 15211–15222 (2023) [2](#), [4](#)
71. Zhang, X., et al.: Pmc-vqa: Visual instruction tuning for medical visual question answering. arXiv preprint arXiv:2305.10415 (2023) [3](#)
72. Zhou, K., et al.: Conditional prompt learning for vision-language models. In: CVPR. pp. 16816–16825 (2022) [2](#), [4](#), [9](#), [10](#)
73. Zhou, K., et al.: Learning to prompt for vision-language models. IJCV **130**(9), 2337–2348 (2022) [2](#), [3](#), [4](#), [8](#), [9](#), [10](#)
74. Zhu, B., et al.: Prompt-aligned gradient for prompt tuning. In: ICCV. pp. 15659–15669 (2023) [2](#), [7](#)